

## CHARACTERIZING THE PHOTOMETRIC RESPONSE OF THE ANS COLLABORATION MONITORING PROGRAM

U. Munari<sup>1</sup> and S. Moretti<sup>2</sup>

<sup>1</sup> *ANS Collaboration, c/o Astronomical Observatory, Asiago, Italy*

<sup>2</sup> *INAF Astronomical Observatory of Padova at Asiago, Italy*

Received: 2011 December 2; accepted: 2011 December 15

**Abstract.** The ANS Collaboration uses the  $UBVR_CI_C$  filters from various commercial manufacturers (Omega Optical, Custom Scientific, Schuler, Optec, Astrodon) for its ongoing photometric monitoring of symbiotic stars. We measured their transmittance profiles over the range 2000 Å to 1.1 μm for various operating conditions, and we are monitoring their evolution over time. Their field performance in terms of color equations has been evaluated by analyzing the transformations from local to standard system of the 14602 observing runs so far collected on symbiotic stars with the ANS Collaboration telescopes. Ageing effects, red leaks and transmittance vs. angle of incidence are also evaluated.

**Key words:** stars: symbiotic binaries, novae – photometry

### 1. INTRODUCTION

For the transformation of photometric measurements in the local (sometimes called as instrumental) systems to the standard system, the method of color equations is usually used. These equations can be determined using a set of standard stars widely distributed in color.

One essential ingredient in shaping the passband profiles of a local photometric system is the transmittance of the filters in use. There are many commercial manufacturers offering partial or complete sets of photometric filters, with size and housing appropriate for commercially available filter wheels. The vendors, however, rarely supply the filter sets with transmittance curves measured for the given specimen. If this happen, the data are usually provided only in a graphical form and are limited to a restricted wavelength range of nominal filter transmittance, leaving undocumented the wavelength regions where red or blue leaks could be present. Furthermore, in the rare cases when tabular transmittance profiles are provided, the angle of incidence of the radiation is left unspecified or is limited to the condition of normal incidence. Finally, filters, and especially their coatings, may suffer from ageing effects (e.g. hygroscopic deterioration), and they need to be monitored over time.

For these and other reasons, pursuing high quality standards, the ANS Collaboration decided to carry out its own investigation of the filter sets mounted on its telescopes, and to monitor the evolution over time of them in a long use. The aim of this paper is to review some of the observed characteristics of color-equations,

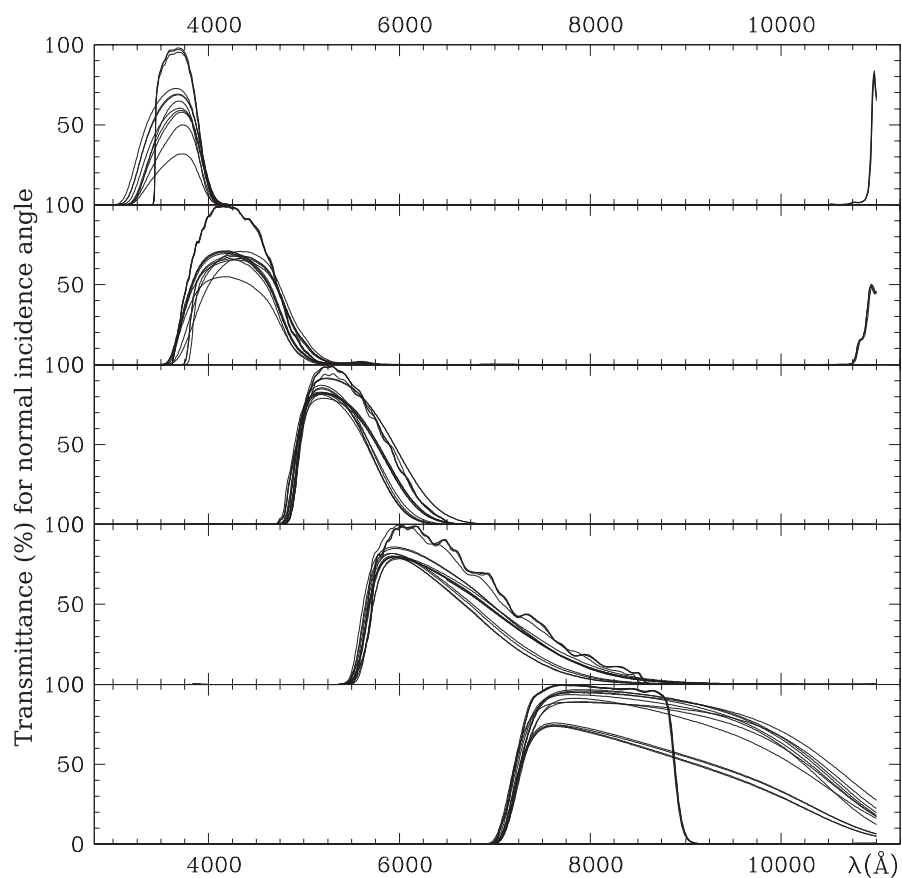


**Fig. 1.** The transmittance curves (for  $90^\circ$  incidence angle) measured for a sample of the photometric filters in use in the ANS Collaboration telescopes.

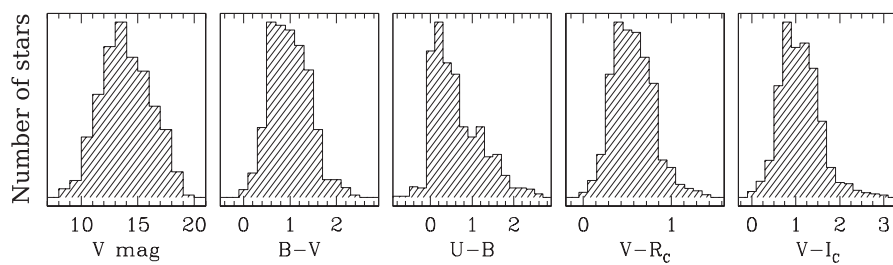


**Fig. 2.** Distribution in magnitude and color of the 912 Henden & Munari (2000, 2001, 2006) photometric standards around 81 symbiotic stars.

**Table 1.** Mean values and dispersions for the distributions in Figure 3.

	Schuler		Custom		Astrodon		Omega		Optec	
	Mean	$\sigma$	Mean	$\sigma$	mean	$\sigma$	Mean	$\sigma$	Mean	$\sigma$
$\alpha(B)$	-0.004	0.102	0.194	0.099	0.012	0.069	0.243	0.065	-0.013	0.058
$\alpha(V)$	0.001	0.050	-0.054	0.033	0.023	0.070	-0.017	0.057	-0.020	0.065
$\alpha(R_C)$	-0.019	0.046	-0.068	0.032	-0.000	0.044	-0.043	0.067	-0.043	0.048
$\alpha(I_C)$	0.016	0.050	0.020	0.035	0.005	0.086	0.049	0.069	0.019	0.047
$\beta(B-V)$	1.002	0.098	0.779	0.065	1.011	0.058	0.778	0.046	1.015	0.038
$\beta(V-I_C)$	1.011	0.058	1.074	0.068	0.989	0.069	1.075	0.047	1.015	0.066
$\beta(V-R_C)$	0.953	0.098	0.973	0.068	0.969	0.081	0.956	0.061	0.853	0.055
$\beta(R_C-I_C)$	1.096	0.119	1.195	0.096	1.011	0.107	1.203	0.063	1.187	0.079

field use and transmittance profiles of the  $UBVR_CI_C$  filter sets operated by ANS Collaboration.

## 2. FILTER TRANSMITTANCES

As it is detailed in Munari et al. (2012), the ANS Collaboration runs a number of different types of telescopes and coatings (refractors, Cassegrains, Newtons, Schmidts), equipped with a broad variety of CCD cameras (like Starlight, SBIG, HiSis, Apogee, FLI, Tektronix, Moravian, Andor), placed at various altitudes from sea-level to mountain tops, and containing photometric filter sets from various companies: Schuler, Custom, Omega, Optec and Astrodon. The first four are classical sandwiches of colored glasses, like those used by Landolt (1983, 1992) and standardized by Bessell (1990). In Astrodon filters, the shaping of the transmittance bands is achieved by the dielectric multi-layer technology.

To measure the transmittance profiles of the filters, we used a Perkin Elmer UV-Vis spectrometer Lambda Bio 40 operated by the ARPA laboratory of Forlì (Italy). Each filter was measured at the room temperature over the whole range from 2000 Å to 1.10  $\mu\text{m}$ , with readings every 10 Å. The light beam had a diameter of 7 mm and was aimed at the geometrical center of the filter (a few scattered tests, comparing with readings taken away from the geometrical center of the filter, provided negligible differences). Figure 1 presents a sample of the obtained transmittance curves.

The filters to be measured were taken down from various telescopes and handled to the laboratory in conditions as close as possible to those at the telescope. At the laboratory, they were measured as received. Only after this first measurement, the filters were carefully cleaned with coating-preserving materials and measured the second time. The difference between these two sets of readings quantified the cumulative effect of their actual use at the given telescope.

## 3. THE REFERENCE STANDARD SYSTEM

The ANS Collaboration measurements of 81 symbiotic stars were calibrated via the  $UBVR_CI_C$  photometric sequences defined in their surroundings by Henden & Munari (2000, 2001, 2006). These sequences represent the local realization of

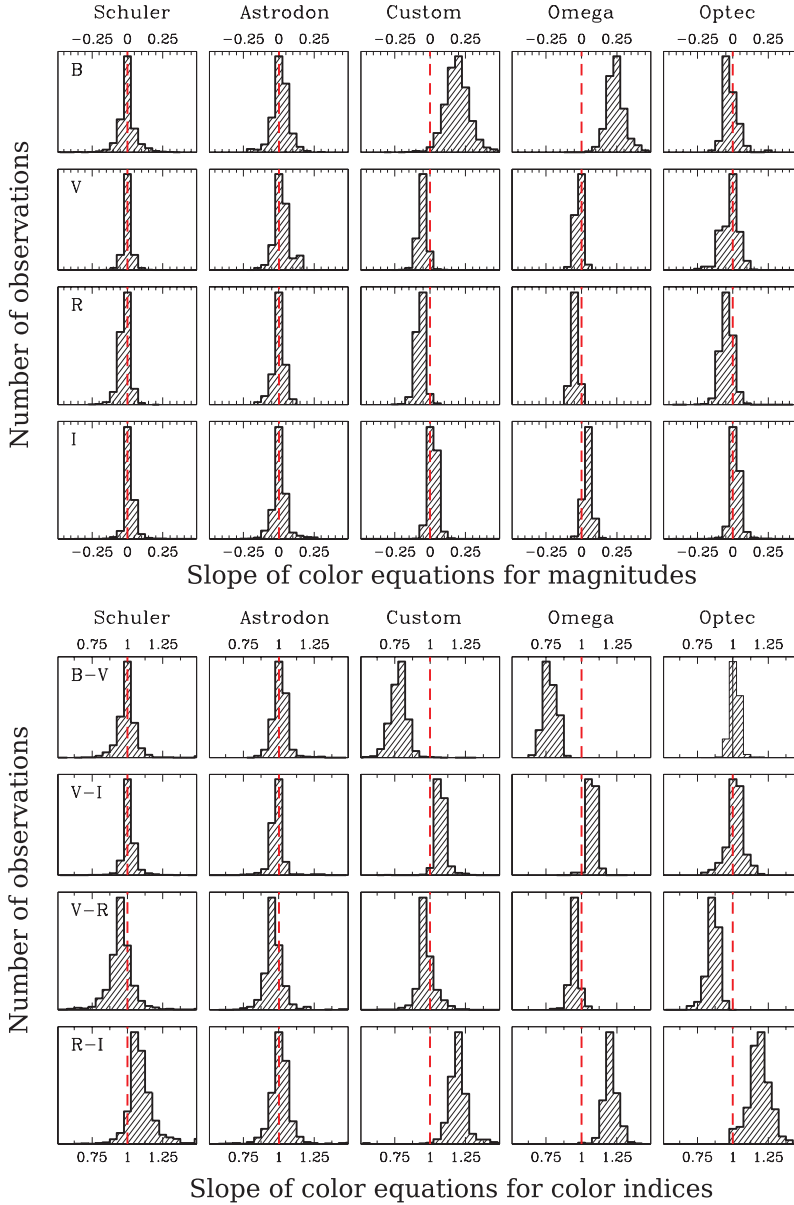


**Fig. 3.** Distribution of  $\alpha$  and  $\beta$  values of Eq. (1) color-equations for 14602  $BVR_{CI}$  measurements of symbiotic stars collected by the ANS Collaboration telescopes between 2005–2011. They are grouped according only to filter type, and include all measurements collected with that type of filter irrespective of the target star, telescope type, altitude, airmass, CCD type, sky condition, Moon phase, etc.

the Landolt (1983, 1992) system of equatorial standards, and were measured via extensive observations with the US Naval Observatory 1.0 m reflector. The Henden & Munari local sequences therefore represent the *standard* system of reference for observations of the ANS Collaboration. The distributions in magnitude and color of the 912 stars defining Henden & Munari local photometric sequences are presented in Figure 2, which also defines the range of color validity for the analysis of the filters considered in this paper.<sup>1</sup>

#### 4. RESULTS

Over the linear range, the transformation equations of between magnitudes and colors of the local system and of the standard system takes the usual form:

$$\begin{aligned}
 U &= u + \alpha_u \times (u - b) + \gamma_u , & U - B &= \beta_{ub} \times (u - b) + \delta_{ub} , \\
 B &= b + \alpha_b \times (b - v) + \gamma_b , & B - V &= \beta_{bv} \times (b - v) + \delta_{bv} , \\
 V &= v + \alpha_v \times (v - i) + \gamma_v , & V - R_C &= \beta_{vr} \times (v - r) + \delta_{vr} , \\
 R_C &= r + \alpha_r \times (v - i) + \gamma_r , & V - I_C &= \beta_{vi} \times (v - i) + \delta_{vi} , \\
 I_C &= i + \alpha_i \times (v - i) + \gamma_i , & R_C - I_C &= \beta_{ri} \times (r - i) + \delta_{ri} .
 \end{aligned} \tag{1}$$

where  $\alpha$  and  $\beta$  are slopes, and  $\gamma$  and  $\delta$  are constants. Capital letters refer to the standard system, lower-case letters – to the local system. The local magnitudes and colors are defined by the instrument (entire optical train), reference photometric sequence and the atmosphere. When the local system completely coincides with the standard one, the values of the coefficients are  $\alpha=0$  and  $\beta=1$ .

Over the period from 2005 July 1 to 2011 July 1, within the ANS Collaboration we logged 14602  $BVR_CI_C$  photometric runs of symbiotic stars, each of them providing a separate value of the coefficients  $\alpha$  and  $\beta$  in Eq. (1). Only a small fraction of these runs included also the  $U$  passband, and because any related statistics would be based on small numbers, the  $U$  band is dropped from the rest of this paper.

Figure 3 presents the distribution of  $\alpha$  and  $\beta$  values of Equations (1) according to the filters brand, without any selection based on target star, telescope, altitude, airmass, CCD type, sky conditions, Moon phase, etc. The distributions in Figure 3 are sharp and resemble symmetric Gaussians, with the values of  $\alpha$  and  $\beta$  close to 0.0 and 1.0, respectively, which guarantee a fair quality of the transformation from the local to the standard system. Significant color terms are present only for the Custom Scientific and Omega Optical  $B$  filters and the corresponding  $B-V$  color indices, and for the Custom, Omega and Optec  $R_C-I_C$  indices.

The distributions in Figure 3 sharpen significantly when only one instrument, working on the same single star, is considered. For example, the left part of Figure 4 presents the same type of data as Figure 3, but limited to a single instrument (in this case R030: a Meade RCX 400 + SBIG ST-9 + Omega Optical  $B$  filter and Custom Scientific  $VRC_I_C$  filters) and a single star (V471 Per, 452 observations in 5 years), without restrictions on airmass or sky conditions. The

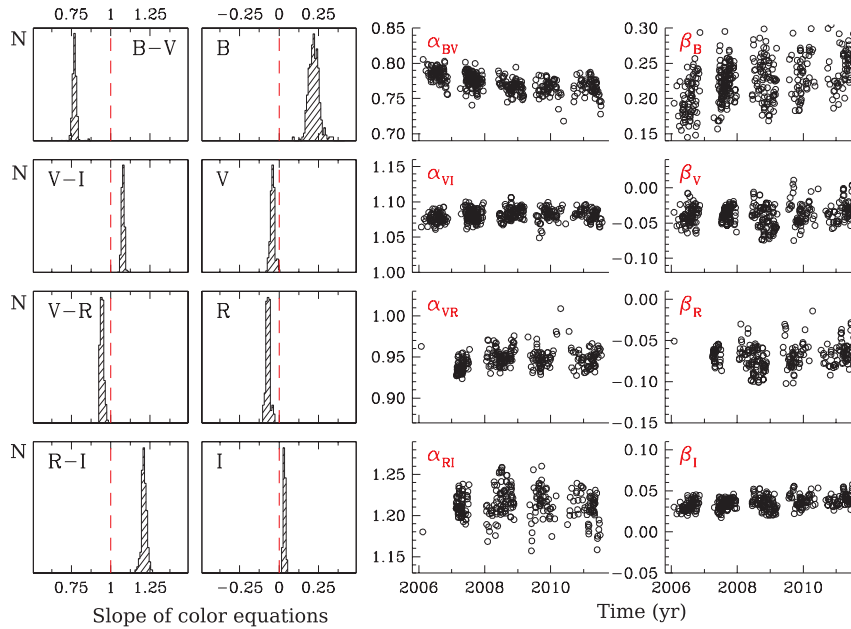
---

<sup>1</sup>Disclaimer: this paper aims to present a methodology, and by no means ranking the performances of the filters under study. The results presented here may not be applicable to other instruments/telescopes, or research/observation applications, or realization of the Johnson-Cousins system other than Landolt's one, or to other sets of filters from the same manufacturers, especially those produced at later times and with different recipes/technologies than those considered here.

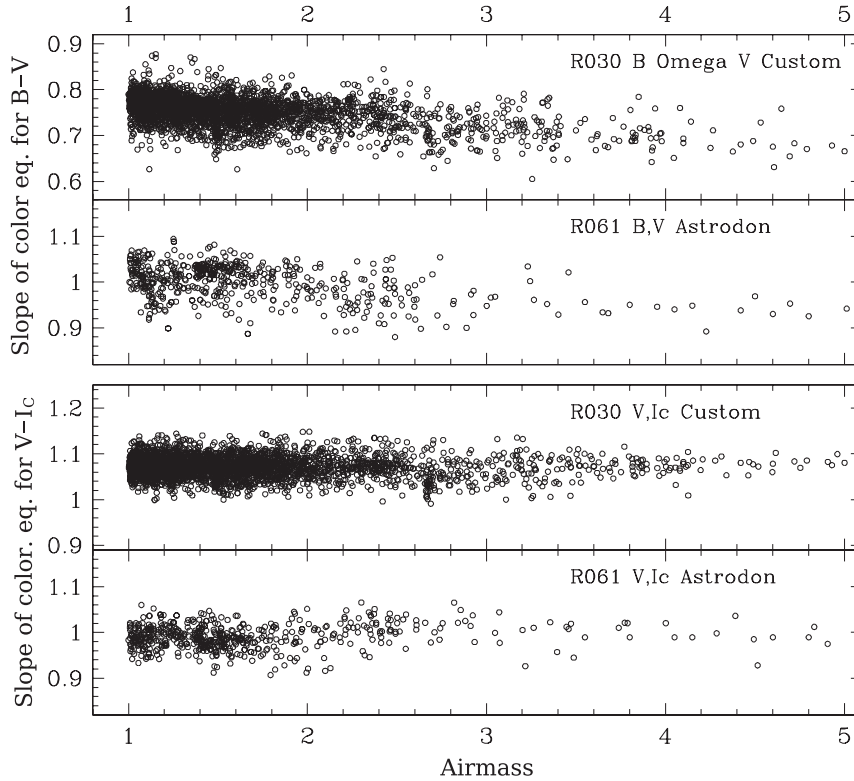
resulting very sharp Gaussian distributions are characterized by essentially negligible dispersions:  $\sigma_{B-V}=0.017$ ,  $\sigma_{V-I}=0.008$ ,  $\sigma_{V-R}=0.012$ ,  $\sigma_{R-I}=0.018$ ,  $\sigma_B=0.038$ ,  $\sigma_V=0.014$ ,  $\sigma_R=0.014$ ,  $\sigma_I=0.006$ . The distribution for the  $B$  passband in Figure 4 stands apart from the rest. The displacement from the ideal 0.0 value, and the high number of measurements taken at great airmasses inflate its width. However, these are not the only reasons. The right part of Figure 4 plots the same data as the left part but against the observing date. The  $B$  filter shows an obvious time dependence, a sign of ageing, with the time dependence for  $I_C$  filter being quite small and those for  $V$  and  $R_C$  close to zero. Removing the time trend from the left panels in Figure 4 provides twice sharper distributions for  $B$  and  $B-V$ .

The ANS Collaboration observations are scheduled to minimize the effect of seasonal conjunction of targets with the Sun. This may require to catch a target quite low to the horizon, just after sunset or shortly before dawn. The presence of standard photometric sequences around all targets, minimizes the effects of high airmasses and in particular of local atmospheric nonhomogeneities. As an example, Figure 5 plots airmass against the value of  $\beta_{B-V}$  and  $\beta_{V-I}$  for all the data collected with two telescopes, irrespective of targets and sky conditions. Both  $\beta_{V-I}$  distributions do not show any trend with airmass (the same is for  $\beta_{V-R}$  and  $\beta_{R-I}$ ), and those for  $\beta_{B-V}$  are small and nearly identical between the two instruments.

Traditional use of astronomical filters places them normal to the incident light, or closely so, as in the long focus/slow focal ratio instruments, or even in a parallel



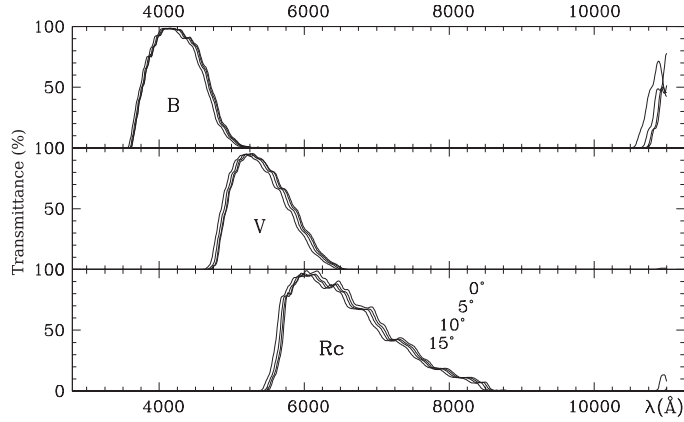
**Fig. 4.** The left panels exhibit the distribution in colors and magnitudes of 452 observations of the symbiotic star V471 Per collected during 5 years with the telescope R030. The right panels exhibit the coefficients of color equations where some effects of ageing of the filters are seen.



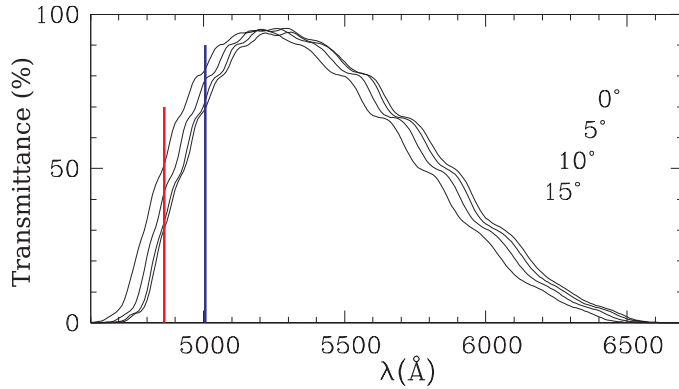
**Fig. 5.** Dependence of the  $\beta$  slopes of Eq. (1) color-equations on airmass for two of the ANS Collaboration telescopes. A dependence on airmass is present for  $B-V$  and it is negligible for  $V-I_C$  (and for  $V-R_C$  and  $R_C-I_C$  as well). The plots for other ANS instruments are similar.

beam as in present-day imager/spectrographs. This is the way in which also the ANS Collaboration uses its own filters, the typical  $f$ /ratio of its instruments being 10. However, the illumination of filters in fast-focal ratio and wide-field telescopes the angles of incidence can be different from the normal, and this is surely the case for filters placed *in front* of objective lenses in patrol cameras. The transmittance profile of traditional filters (sandwich of colored glasses) change very little for moderate angles away from normal incidence, being proportional to the projected light-travel within the glass which goes as  $\approx 1/\cos \theta$ . In multi-layer dielectric filters, the change of the transmittance profile with the illumination angle is much faster and characterized by almost a rigid shift toward shorter wavelengths. Figure 6 presents our measurement of the change in the transmittance profile for the set of Astrodon multi-layer filters in use with the ANS Collaboration telescope R122. The shift toward bluer profiles is evident (the red leaks follow the same pattern).

This shift toward shorter wavelengths may induce large differences in the measurements when dealing with strong emission line objects, similar to novae and many symbiotic stars. Figure 7 zooms into the  $B$  filter transmittance curves of



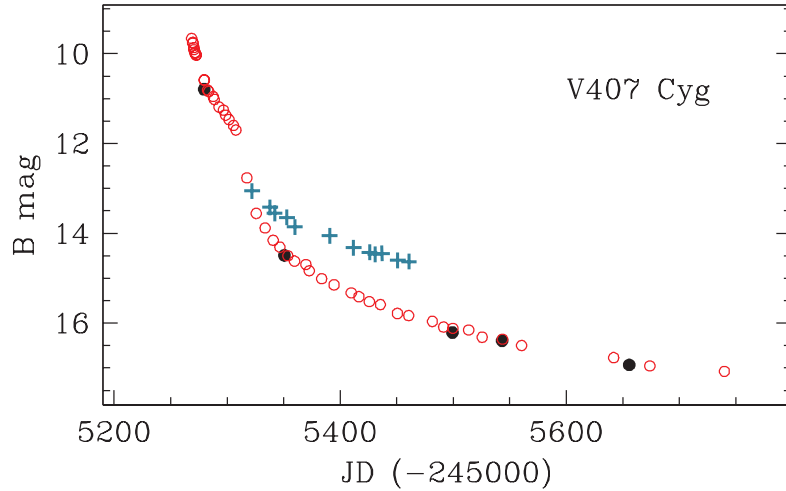
**Fig. 6.** Dependence of the filter transmittance on the angle of incident light for the Astrodon filters which are in use at the ANS Collaboration telescope R122 (the quoted angles are deviations from the normal incidence).



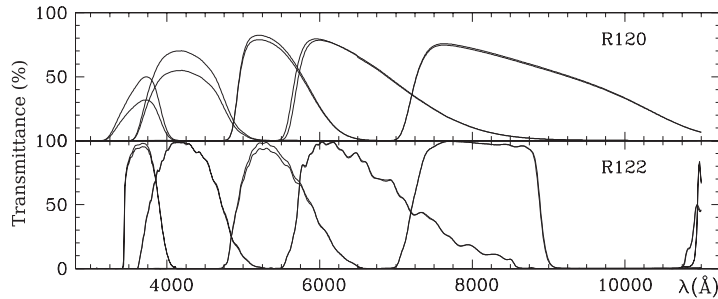
**Fig. 7.** Zooming on the V passband filter of Figure 6. The two vertical lines mark positions of the  $H\beta$  and [O III] 5007 Å lines.

Figure 6. Moving  $15^\circ$  away from the normal incidence doubles the transmitted flux for  $H\beta$  and increases by  $\sim 20\%$  the flux for [O III].

Figure 6 shows another potential problem of multi-layer dielectric filters, the presence of red-leaks. The sensitivity of commercial CCDs declines smoothly into the far red, and at  $\lambda \geq 1 \mu\text{m}$  they are quite insensitive but not yet completely blind. A very red object combined with a red-leaking filter can trigger response from the CCD sensitivity tail beyond  $1 \mu\text{m}$ . This is exactly what happened during the 2010 outburst of V407 Cyg, as illustrated in Figure 8. During the outburst decline, the blue emission from outbursting WD + nebular material steadily reduced in comparison with the stable emission from the cool giant companion. When V407 Cyg reddened to  $V-I_C \geq 3.8$ , the fraction of light recorded through the B band red-leak became non-negligible with respect to what was going through the normal transmittance profile, and the measurements taken with the R061 instrument



**Fig. 8.** The effect of the red leak of multi-layer filters when observing very red stars, like V407 Cyg during the return to quiescence following its 2010 outburst. Magnitudes  $B$  from the ANS telescope R061 (crosses), equipped with Astrodon filters, deviated from those of the telescopes equipped with classical colored glass filters (open and filled circles) when  $V-I_C$  turned  $\geq 3.8$ .



**Fig. 9.** *Top panel.* Transmittance of the Schuler filters of the ANS telescope R120 before and after cleaning (after a year of normal use). *Bottom panel.* The change in transmittance of the Astrodon filters of the ANS telescope R122 after 18 months of normal use (both sets of curves before cleaning).

(crosses in Figure 8) went progressively deviating from those of other instruments equipped with classical glass filters (open and solid circles). We are glad to note that private communication from Astrodon suggests that these red-leaks will be soon suppressed in future production. These leaks may affect the measurements of only the reddest stars, a truly small fraction even among the 81 symbiotic stars under monitoring by the ANS Collaboration.

Figure 9 illustrates the typical effects of weathering to filter surfaces using them for a long time at the sea level and high humidity conditions. This damage of filters usually is removable by accurate cleaning.

Finally, a careful inspection of accurate, high S/N transmittance profiles of

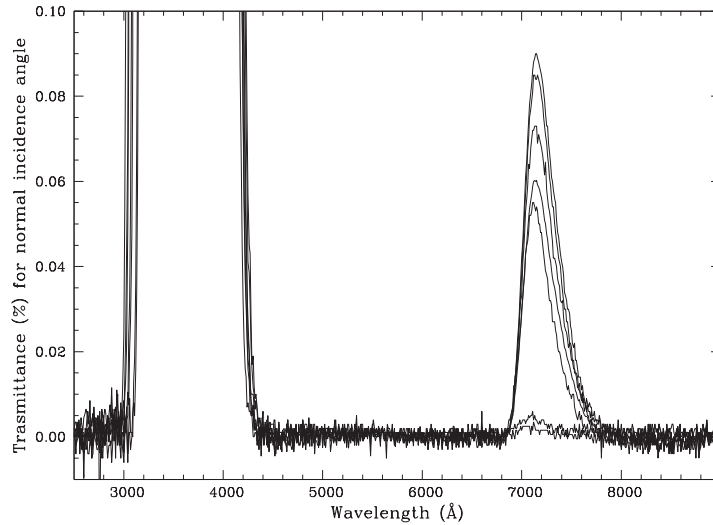


**Fig. 10.** Transmittance of some *U* filters from the classical sandwiches of colored glasses variety replotted from Figure 1 at a much stretched ordinate scale. Note the varying effectiveness of Schott UG 2 glass in suppressing the red leak longward of 685 nm.

filters may reveal subtle features. For example, in Figure 10 we replot at a much stretched ordinate scale some of the transmittance profiles of *U* filters from Figure 1. The replotted filters are of the classical sandwiches of colored glasses variety. It is evident from Figure 10 how different is the effectiveness in suppressing completely the red-leak of the Schott UG1 color glass longward of 685 nm with Schott BG 39 glass, presumably caused by minimal differences in the effective thickness of glasses. For a M2 III star, the difference in the total flux transmitted by a filter with or without the strongest red-leak in Figure 10 amounts to 0.067 mag.

## REFERENCES

- Bessell M. S. 1990, *PASP*, 102, 1181  
 Henden A., Munari U. 2000, *A&AS*, 143, 343  
 Henden A., Munari U. 2001, *A&A*, 372, 145  
 Henden A., Munari U. 2006, *A&A*, 458, 339  
 Landolt A. U. 1983, *AJ*, 88, 439  
 Landolt A. U. 1992, *AJ*, 104, 340  
 Munari U. et al. 2012, *Baltic Astronomy*, 21, 13 (this issue)